The Journal of Adhesion

ISSN: 0021-8464 (Print) 1545-5823 (Online) Journal homepage: http://www.tandfonline.com/loi/gadh20

Effect of an Atmospheric Pressure Plasma Treatment on the Mode I Fracture Toughness of a Co-Cured Composite Joint

J. Mohan , A. Ramamoorthy , A. Ivanković , D. Dowling & N. Murphy

To cite this article: J. Mohan , A. Ramamoorthy , A. Ivanković , D. Dowling & N. Murphy (2014) Effect of an Atmospheric Pressure Plasma Treatment on the Mode I Fracture Toughness of a Co-Cured Composite Joint, The Journal of Adhesion, 90:9, 733-754, DOI: 10.1080/00218464.2013.772053

To link to this article: https://doi.org/10.1080/00218464.2013.772053

Accepted author version posted online: 28 Feb 2013.
Published online: 28 Feb 2013.

The Journal of Adhesion, 90:733–754, 2014

ISSN: 0021-8464 print/1545-5823 online
DOI: 10.1080/00218464.2013.772053

Taylor & Francis
Taylor & Francis Group

Effect of an Atmospheric Pressure Plasma Treatment on the Mode I Fracture Toughness of a Co-Cured Composite Joint

J. MOHAN, A. RAMAMOORTHY, A. IVANKOVIĆ, D. DOWLING, and N. MURPHY

Centre of Adhesion and Adhesives, School of Mechanical and Materials Engineering, University College Dublin, Belfield, Dublin, Ireland

In this study, the surface of a composite prepreg was treated using an atmospheric pressure plasma in an attempt to improve the fracture toughness of a co-cured joint system. Three gas mixtures were investigated; helium, helium/nitrogen, and helium/oxygen. The processing parameters of the system were varied to obtain the maximum increase in surface energy of the prepreg. A He/O_2 plasma was found to be the most efficient treatment, giving the largest increase in surface energy in the shortest time. Co-cured joints were then fabricated using prepreg that had been treated with various plasmas. A modest 15–18% increase in the Mode I fracture toughness was achieved. However, the locus of failure remained interfacial. It was also observed that a He/O_2 plasma treatment could be detrimental to joint toughness for long treatment times.

KEYWORDS Composites; Fracture mechanics; Surface treatment by excited gases (e.g., flame, corona, plasma)

1. INTRODUCTION

When composites and adhesives are used to manufacture large parts in the aerospace industry, it is often convenient to co-cure the two materials using a single processing operation. This helps to reduce the high costs associated with autoclave curing and also to reduce processing time. However, despite

Received 13 November 2012; in final form 29 January 2013.

Address correspondence to N. Murphy, Centre of Adhesion and Adhesives, School of Mechanical and Materials Engineering, University College Dublin, Belfield, Dublin 4, Ireland. E-mail: Neal.Murphy@ucd.ie

Color versions of one or more of the figures in the article can be found online at www.tandfonline.com/gadh.

the apparent advantages, co-curing is not without its drawbacks. Epoxy resins have been shown to contain small quantities of both free and bound water [1]. This moisture is then released during the curing process, causing plasticisation of the adhesive as well as interfacial failure due to the presence of voids at the adhesive-substrate interface [2,3].

Plasma treatments have been shown to be extremely versatile in pre-treating a wide variety of polymer and composite substrates for adhesive bonding [4]. For example, adhesion to carbon-fiber/bismaleimide [5], carbon-fiber/polyether ether ketone (PEEK) [6,7], glass-fiber/nylon 6,6 [8], glass-fiber/polyester [9], and carbon-fiber/epoxy [10–14] composites have all been improved through the use of plasma treatments. However, careful selection of the processing parameters is required as too long a treatment can be detrimental to the joint strength [12,15].

Plasma treatments tend to introduce oxygen-containing functional groups onto the composite surface [6,9,16]. This aids wettability of the adhesive and improves bond strength [11,12]. Plasma treatments also have the added benefit of removing mould release agents from the composite substrate which can impede adhesion [5,13]. The chemical changes induced on the surface of the composite material through the use of plasma treatments have been shown to be stable for up to 90 days after treatment [6].

There has been a considerable amount of work published on the use of plasma treatments in the adhesive bonding of composites. However, most of this work has been concerned with secondary bonded joints. Although prepregs have been plasma treated [17], this was only for improving delamination fracture toughness and co-cured joints were not considered. The atmospheric pressure plasma treatment of a composite prepreg for use in a co-cured joint will be investigated in this work.

2. MATERIALS & METHODS

2.1. Manufacture of Co-Cured Composite Joints

Two aerospace grade materials were used in the present study; a 177°C cure unidirectional carbon-fiber/epoxy prepreg (CYCOM 977-2/HTS) and a dual 120/177°C cure epoxy film adhesive (FM300-2M). Both materials were manufactured and supplied by Cytec Engineered Materials (CEM) (Harve de Grace, Maryland, USA).

The co-cured joints were produced in-house at University College Dublin (UCD) using a vacuum bagging layup procedure similar to that used in industry. Each substrate consisted of 10 plies of 977-2/HTS prepreg. A 12-μm, thick PTFE sheet was placed between the prepreg and adhesive on one side of the layup to act as a crack initiator. Co-cured joints were produced by curing the prepreg and the adhesive at the same time in a single process operation at 177°C. Once cured, the bonded composite laminates

were machined to size using a diamond grinding disc. The specimens were cut to a nominal width of 25 mm and length of 150 mm with an initial crack starter length of 45 mm from the load-line. The total thickness of each specimen was ≈5.6 mm with an adhesive layer thickness of ≈0.25 mm.

2.2. Fracture test Methods

Double cantilever beam (DCB) tests were conducted in accordance with the British Standard **7991** [18]. An illustration of the DCB specimen, with key components highlighted, can be seen in Fig. 1a. A Tinius-Olsen (Horsham, Pennsylvania, USA) Hounsfield 50 K screw-driven tensile test machine was used for the fracture tests. A 10 kN load cell was used to record the applied load. The crack length was monitored using a travelling microscope with ×10 magnification. All tests were carried out at a constant crosshead displacement rate of 1 mm/min at room temperature. The specimens were held in place using load blocks and loading pins as shown in Fig. 1b. Three repeats were performed for each treatment. The propagation fracture toughness, G_{IC}, was calculated using a corrected beam theory (CBT) analysis from Eq. (1):

$$G_{IC} = \frac{3P\delta}{2B(a+\Delta_I)} \cdot \frac{F}{N}, \tag{1}$$

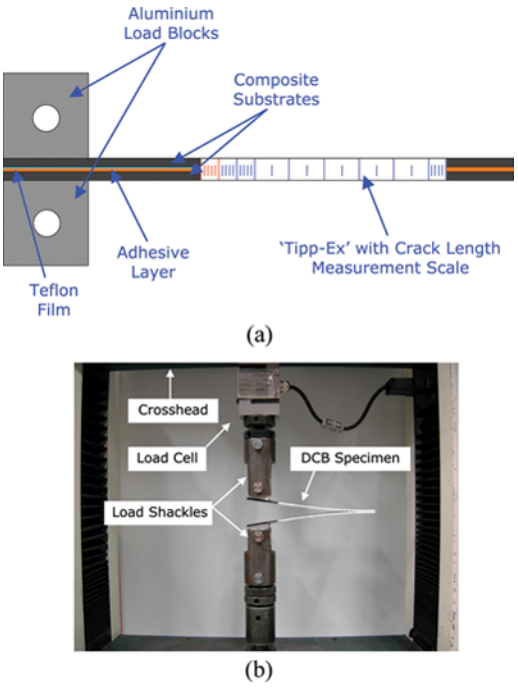

Figure 1 Illustrations and photographs of DCB experimental setup. (a) DCB Illustration and (b) DCB photo.

where P is the load, δ, the opening displacement, B is the width of the specimen, and a is the crack length. F, N, and Δ_I are correction factors for large displacements, load block effects, and root rotation of the crack tip, respectively. They are based on several papers by Williams [19–21] and are also detailed in [18].

2.3. Scanning Electron Microscopy Method

Scanning electron microscopy (SEM) was performed on the adhesive-substrate interfaces and treated prepreg surfaces using a Hitachi (Krefeld, Germany) TM-1000 Tabletop-Microscope. The samples were gold coated prior to imaging to reduce charging.

2.4. Thermal Characterisation Methods

Thermal characterisation was performed on a Rheometric Scientific (Surrey, United Kingdom) STA 1500. Small samples of material were placed in a 6-mm diameter aluminium crucible. An empty crucible was used as a reference sample for differential thermal analysis (DTA). The samples were kept in a flowing nitrogen atmosphere throughout the analysis and heated from 25 to 350°C at a rate of 10°C/min. These dynamic scans were used to determine the glass transition temperature of the adhesive material taken from the fractured specimens.

2.5. Surface Energy Characterisation

Surface energy characterisation was performed on a Data Physics (Filderstadt, Germany) OCA 20 system with video capture apparatus. Three probe liquids (deionised water, diiodomethane, and ethylene glycol) were used in the surface energy characterisation. The Sessile drop technique was used in the present work. Three 1-μL drops of each liquid were placed on the prepreg surface for repeatability (i.e., three surface energy measurements were taken for each treatment). The contact angle between each drop and the substrate was measured using the accompanying system software. The surface energy of the composite was calculated based on the Owens, Wendt, Rabel, and Kaelble (OWRK) method [22]. The properties of the probe liquids were taken from Strom *et al.* [23].

Recently, the limitations of the sessile drop technique were discussed in an essay by Strobel and Lyons [24]. The authors advocated the importance of measuring both the advancing and receding contact angles as opposed to just the static values obtained from the sessile drop technique. If the surface exhibits a large degree of hysteresis (*i.e.*, difference between the advancing and receding contact angles) then the static value could potentially be any value in-between. With this in mind, the sessile drop technique utilised in the present work should be viewed as a means for comparing relative changes

in different surface treatments (as noted by Müller and Oehr [25] in their response to Strobel and Lyons [24].)

2.6. Labline™ Plasma Treatment System

Plasma surface pre-treatments were carried out using the Dow Corning (Seneffe, Belgium) Labline™ atmospheric pressure plasma (APP) system, described in [26] and [27]. This machine incorporates a dedicated reel-to-reel web handling system which passes through two sets of parallel-plate electrodes between which a dielectric barrier discharge plasma is formed. (Helium is used to generate the plasma.) The 300×320 mm electrodes consist of a saline salt solution housed in a dielectric perimeter. The system is capable of applying power of up to 2000 W to the electrodes using a generator (frequency circa 20 kHz).

The prepreg specimens were mounted onto a poly(ethylene teraphthalate) support web with double-sided adhesive tape and passed through the plasma at a constant speed of $\approx$1.5 m/min. One pass through both electrodes corresponds to a treatment time of approximately 25 s. The distance between the prepreg specimen and electrode was approximately 2 mm. It should be noted that the APP treatments were only applied to the two prepreg surfaces that were to be in direct contact with the film adhesive.

2.7. Optical Emission Spectroscopy

Optical emission spectroscopy (OES) can be used to gain insight into the atomic and molecular species present in the plasma [28,29]. In the present study, an Ocean Optics (Dunedin, United States) USB4000 UV/VIS spectrometer was used to analyse the spectra of various plasmas. The spectrum was recorded using a fiber optic cable placed between one of the electrode

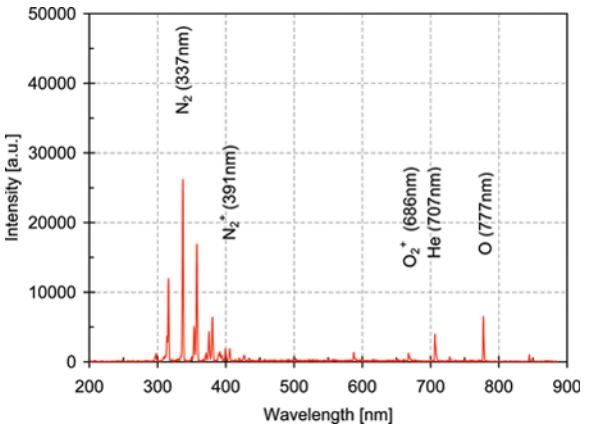

Figure 2 Typical OES spectrum of a He/O_2 plasma at 1600 W.

sets. A more detailed description of the plasma diagnostic techniques, including OES, used on the Labline APP system described in the Section 2.6 is given in [27]. A typical OES spectrum of a He/O_2 plasma at 1600 W is shown in Fig. 2 and a few key species are highlighted. The N_2 peak at 337 nm always has the highest intensity due to the diffusion of air into the He/O_2 atmospheric plasma. Helium (He) and oxygen (O) peaks can be seen at 707 and 777 nm, respectively.

The OES spectra of the species formed in a He, He/N_2, and He/O_2 plasma are given in Fig. 3. The additional oxygen in the He/O_2 plasma

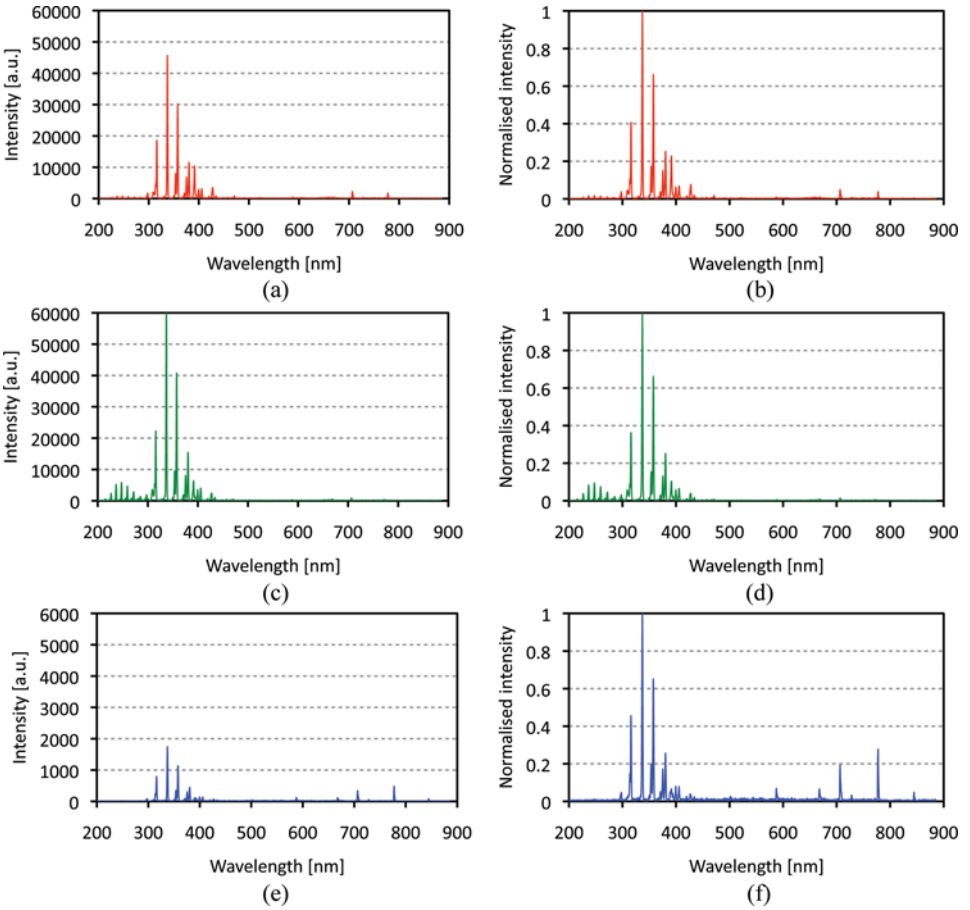

Figure 3 Absolute intensity of OES spectra of the (a) He, (c) He/N_2, and (e) He/O_2 plasmas at 1200 W. Note the scale on the y-axis in (a) and (c) is an order of magnitude higher than (e). The addition of oxygen dramatically reduces the intensity of the spectrum in (e). Intensity ratios of the (b) He, (d) He/N_2, and (f) He/O_2 plasmas at 1200 W. Each spectrum is normalised to the N_2 peak at 337 nm. Note that the He and O_2 peaks at 707 and 777 nm, respectively, in the He/O_2 plasma are now much more prominent. (a) He – Absolute Intensity, (b) He – Intensity Ratio, (c) He/N_2 – Absolute Intensity, (d) He/N_2 – Intensity Ratio, (e) He/O_2 – Absolute Intensity and (f) He/O_2 – Intensity Ratio.

quenches the plasma [27] as evidenced by the considerably lower intensity of the spectrum in Fig. 3e compared to either Fig. 3a or 3c. As expected, the He/N_2 plasma will have a considerably more intense N_2 peak than either a He or a He/O_2 plasma. As a result, it is convenient to normalise the entire spectrum to the intensity of the N_2 peak at 337 nm. This allows the intensity ratios of various peaks to be examined which can give a better insight into the generated plasmas. For example, if the absolute intensity of the O_2 peak from the three gas mixtures is considered (see Fig. 4a), the He plasma would be expected to generate more oxygen containing functional groups on the prepreg surface (*i.e.*, higher surface energy). However, if the intensity ratio of the O_2 peak (*i.e.*, normalised to N_2 peak at 337 nm) is considered (see Fig. 4b), it can be seen that a He/O_2 plasma would lead to more interaction of the oxygen species with the prepreg and, hence, a higher surface energy. As will be seen later, the various gas mixtures employed have very different effects on the resulting surface energy of the treated prepreg. It is expected that the higher intensity ratio of the O_2 peak to the N_2 peak in the He/O_2 plasma will lead to the development of more oxygen-containing polar functional groups and an increased surface energy.

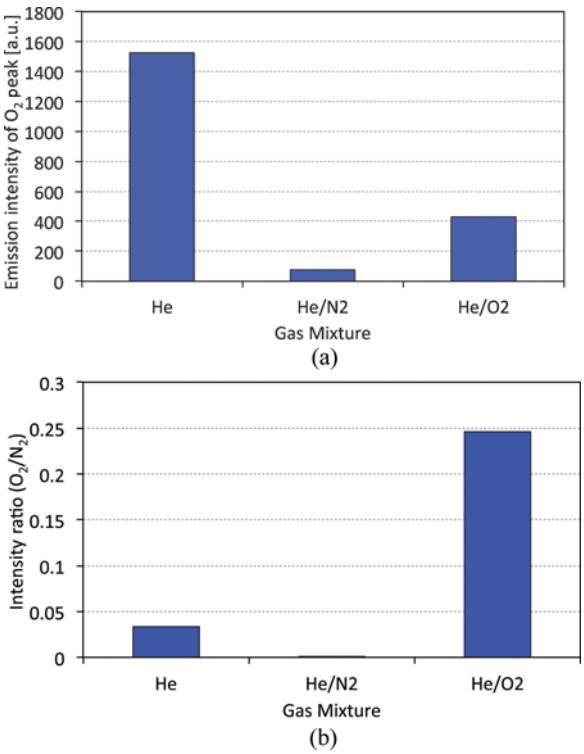

Figure 4 (a) As-measured intensity and (b) intensity ratio (O_2/N_2) of the oxygen peaks from Fig. 3.

Comparing the He/N_2 and He/O_2 plasmas, it was noted that in the case of the former, the nitric oxide (NO) emission bands are observed in the region of 200–300 nm, while these peaks are absent in the case of the He/O_2 plasmas. This absence has been observed previously in other He/O_2 plasma spectra [30,31]. A probable explanation is that the quenching effect of molecular oxygen on the helium plasma results in a very low level of NO being formed.

2.8. X-Ray Photoelectron Spectroscopy

X-ray photoelectron spectroscopy (XPS) analysis was performed to study the chemical composition of the plasma-treated surfaces using a Kratos Analytical (Manchester, United Kingdom) Axis Ultra electron spectrometer equipped with a monochromated Al Kα-ray source. XPS survey spectra were collected in the binding energy range of 0–1200 eV. Photoelectrons were detected at 90° take-off angle (TOA) and the corresponding depth of analysis was 10 nm. Accuracy of XPS is ±2%. The center of the sample was used for the XPS analysis and each result presented in the present work is an average of three measurements taken at different spots.

3. RESULTS AND DISCUSSION

3.1. Surface Energy Analysis

Three different gas mixtures were investigated; helium (He), helium/nitrogen (He/N_2), and helium/oxygen (He/O_2). The He flowrate through the electrodes of the Labline system was maintained at 10 L/min and the concentration of N_2 and O_2 was kept at 2% where applicable. The applied power was fixed at 1200 W and the treatment time was varied up to 40 min. Note that for treatment times greater than 10 mins, the samples were held stationary in the one electrodes rather than being passed back and forth between the two sets of electrodes. The surface energy was measured approximately 2 hrs after treatment. The results for each treatment can be seen in Fig. 5. For clarity, a comparison of the total surface energy in each case is shown in Fig. 6. Each plasma was found to affect the measured surface energy in different ways. Firstly, the He plasma gives a slow steady rise in the polar component with increasing treatment time up to 20 min. There is also a corresponding decrease in the dispersive component. Secondly, the He/N_2 plasma results in similar behavior to the He plasma but on a much smaller scale, only yielding a slight increase and decrease in the polar and dispersive components respectively. Finally, the He/O_2 plasma treatment results in a rapid increase in polar and a decrease in dispersive components after comparatively short treatment times. For the treatment power used, a time of 5 min (12 Passes) is needed to achieve the maximum increase in surface

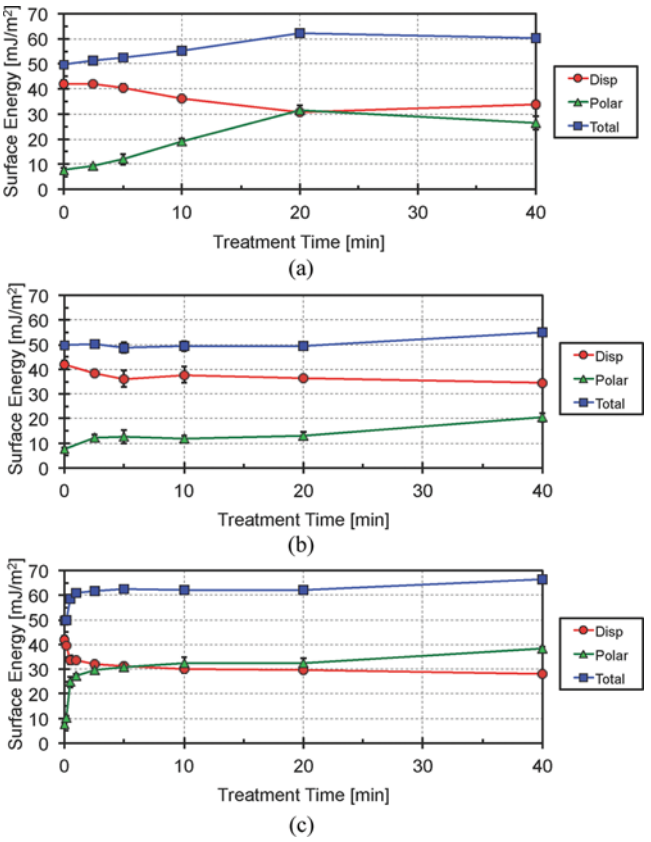

Figure 5 Surface energy results for He, He/N_2, and He/O_2 plasmas at 1200 W as a function of treatment time. These readings were taken approximately 2 hours after treatment. Note that in some cases, the error bars are obscured by the data points. (a) He, (b) He/N_2 and (c) He/O_2.

energy compared to 20 min for a He only plasma. Researchers have attributed the decrease in dispersive component to crosslinking on the material's surface [9,32]. As has been previously shown, the He/O_2 plasma contains

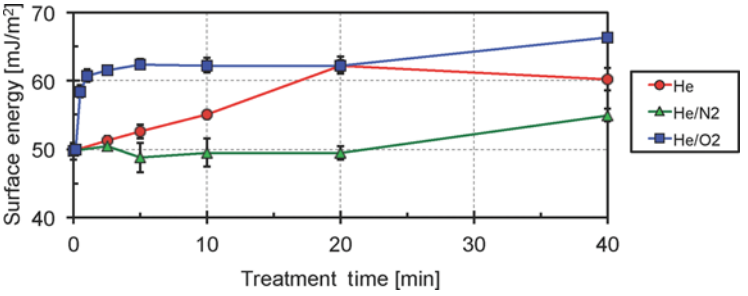

Figure 6 Comparison of total surface energy from Fig. 5. Note that in some cases, the error bars are obscured by the data points.

relatively more oxygen-containing species than a He or He/N_2 plasma [33]. It is believed that this increased concentration of oxygen-containing species in the He/O_2 plasma led to the more efficient increase in surface energy.

An important point to note is that the treatments are being performed on an uncured prepreg material. The polymer chains in the uncured epoxy resin are likely to be highly mobile. To investigate the effect of the different plasmas in more detail, the water contact angle (WCA) was measured in the period immediately after treatment. The prepreg samples were removed from the Labline system and the WCA was monitored up to a time of approximately 1 hr after treatment. Figure 7 shows the WCA of the prepreg after a He, He/N_2, and He/O_2 plasma treatment at 1600 W for 2.5 min (six passes). It can be seen that the He/O_2 plasma results in the greatest reduction in WCA. However, the WCA quickly recovers to approximately 35°within 1 hr of treatment. This is essentially the same value of WCA used in the calculation of the surface energy 2 hrs after treatment as shown in Fig. 5c. It can be seen from Fig. 7 that the He and He/N_2 plasma do indeed give a considerable reduction in WCA in the time immediately after treatment. However, the WCA rapidly recovers to 55°for the He/N_2 plasma which is approximately 85% of the untreated value. The data presented in Fig. 5 therefore represents conservative, stabilised values of prepreg surface energy associated with a variety of plasma treatments.

It has been shown that a He/O_2 plasma is the most efficient for increasing the surface energy of the prepreg material and so it was decided to focus on this treatment. The applied power was then varied from 400 to 1600 W to determine its effect on the surface energy of the treated prepreg. Figure 8 shows the dispersive, polar, and total surface energies of the various treatments with different applied power. A comparison between the total

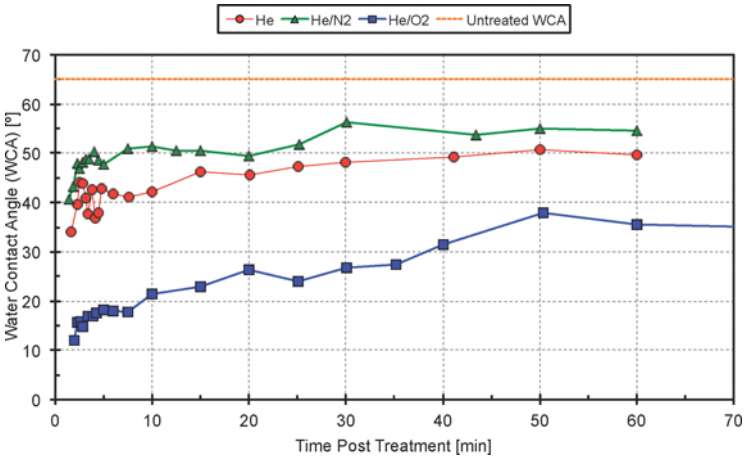

Figure 7 WCA of prepreg immediately after treatment.

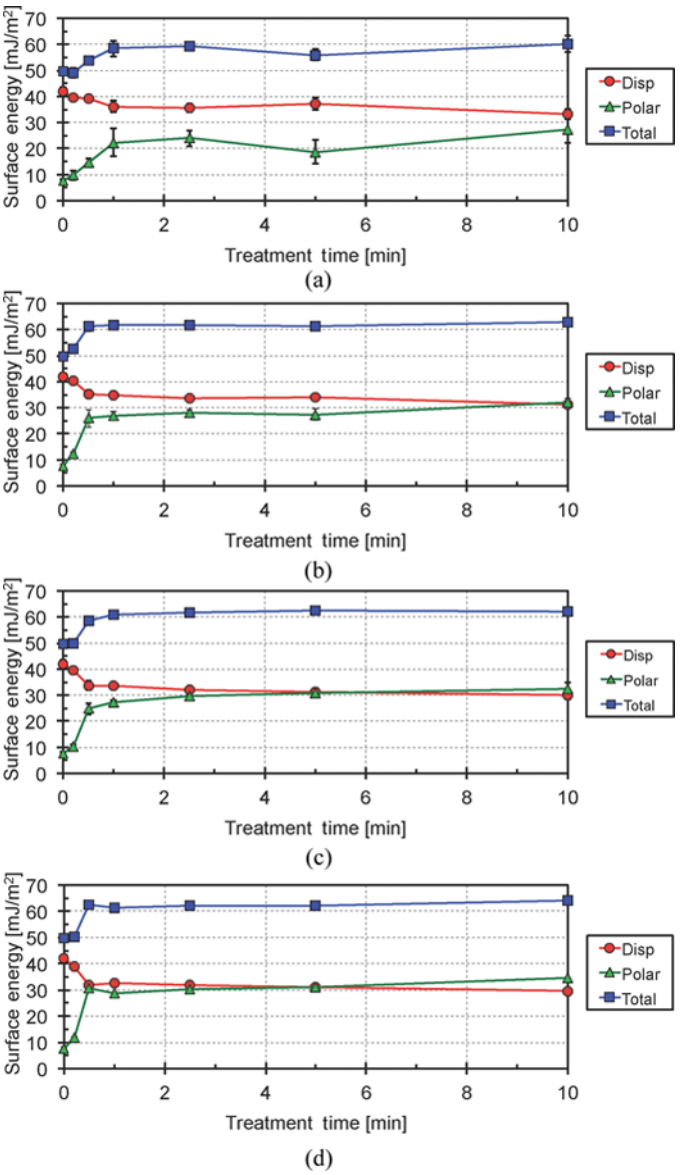

Figure 8 Surface energy results for a He/O_2 plasma at various applied powers and treatment times. Note that in some cases, the error bars are obscured by the data points. (a) 400 W, (b) 800 W, (c) 1200 W, and (d) 1600 W.

surface energy for each applied power is given in Fig. 9. A similar trend of increasing polar and decreasing dispersive components was observed in each case. The higher power levels resulted in a slightly increased final value of surface energy and enabled the maximum effect to be obtained in shorter treatment times. These differences are particularly apparent when comparing

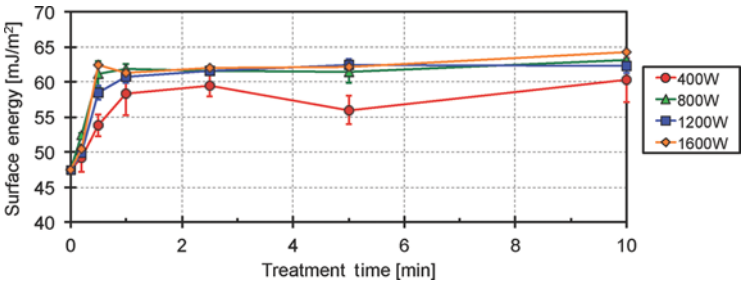

Figure 9 Comparison of total surface energy from Fig. 8. Note that in some cases, the error bars are obscured by the data points.

400 to 800 W but less so at higher applied powers (*i.e.*, 1200 W or 1600 W). The major difference between the higher applied powers evaluated was the reduced scatter in surface energy results at higher power, indicating a more uniform treatment as evidenced by the smaller error bars. In fact, in Fig. 8 the error bars are often obscured by the data points at higher treatment power levels.

The stability of a He/O_2 plasma treatment at 1600 W for 2.5 min (six passes) was investigated by monitoring the surface energy over the course of 28 days. Figure 10 shows that surface energy is stable over the shelf life of the prepreg. There is a modest ($\approx$20%) decrease in the dispersive component over the 28-day period. It should be noted that all co-cured joints produced using activated prepreg were cured within a few hours of plasma treatment.

3.2. Mode I Fracture Toughness

The surface energy results showed that a He/O_2 plasma at 1600 W for 2.5 min (six passes) would yield the largest increase in surface energy in the shortest time. However, for the purpose of this study, the treatment time was still

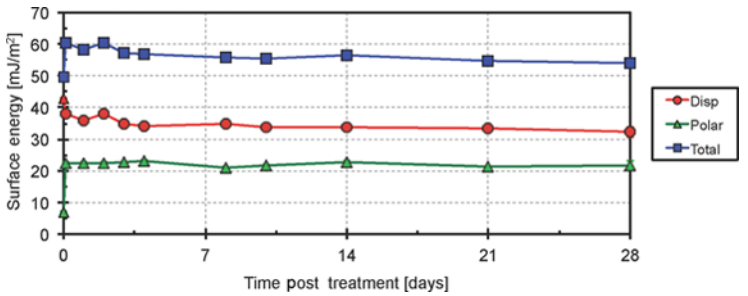

Figure 10 Surface energy of prepreg treated with a He/O_2 plasma up to 28 days after treatment. Note that in some cases, the error bars are obscured by the data points.

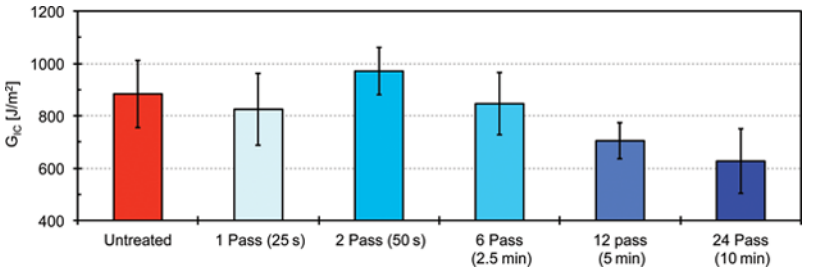

Figure 11 Mode I fracture toughness, G_{IC}, of co-cured joints treated with a He/O_2 plasma. The applied power was constant at 1600 W for all treatments.

varied from 1 to 24 passes to determine its effect. Using these conditions, co-cured joints were produced using APP-treated (atmospheric pressure plasma treated) prepreg. The mode I fracture toughness was determined using the DCB test and the results can be seen in Fig. 11. A slight increase in average toughness for short treatment times (two pass) followed by a more noticeable decrease for longer times (12 & 24 pass) was observed. The results show that only a modest 15–18% increase in the average value for G_{IC} was obtained after a treatment time of two passes (50 s). The locus of failure (*i.e.*, interfacial) remained unchanged regardless of treatment. It should be noted that the error bars overlap to a large extent, particularly when comparing the untreated specimens with samples treated for short treatment times (less than six passes). This is likely due to variations between the samples themselves. For example, even the untreated co-cured joint exhibits a relatively wide scatter. It may also be the case that there were variations in the actual applied plasma treatments. The only definite conclusion that can be drawn is that excessive treatment times result in a weaker joint. It is also interesting to note that despite a treatment time of six passes (2.5 min) giving a large increase in surface energy (see Fig. 8d), the measured fracture toughness was the same as the untreated value.

3.3. XPS Analysis

X-ray photoelectron spectroscopy (XPS) was performed on prepreg samples before and after treatment with a He/O_2 plasma at 1250 W for five passes. The spectra can be seen in Fig. 12. Note that the plasma processing parameter have been modified slightly as they were carried out as part of a second experimental programme. The elemental composition of carbon, oxygen, nitrogen, sulphur, and silicon determined from these spectra is tabulated in Table 1 while the specific functional groups are itemised in Table 2. Note that π-π^* refers to the shake-up satellite and has been previously observed during XPS analysis of plasma treated polymers [34]. It can seen from the XPS results that the He/O_2 plasma has indeed introduced

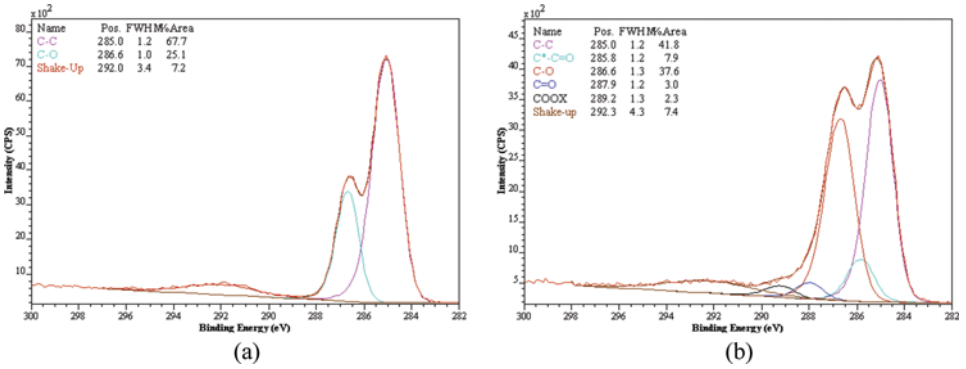

Figure 12 XPS spectra for untreated prepreg and after a He/O_2 plasma treatment. (a) Untreated. (b) He/O_2, 1250 W, and five passes.

oxygen-containing functional groups. This was to be expected given what has already been published in the literature. The presence of sulphur is likely due to either the thermoplastic toughening agent or curing agent found in the Cycom 977-2 resin. The silicon concentration was found to decrease slightly, suggesting that this may be present as a contaminant, which is being partially removed by the plasma treatment. Chin and Wightman [5] observed similar levels of sulphur and silicon on a carbon-fiber/bismaleimide composite during XPS analysis.

3.4. Microscopy and Thermal Analysis

As discussed previously, when the prepreg was treated for long treatment times, the resulting co-cured joints exhibited a reduced fracture toughness. These particular specimens presented slightly different fracture surfaces than tougher samples. While the joints all failed interfacially, the crack path would switch between the two beam arms. When this switching occurs there would have to be some level of cohesive failure that would positively contribute to the measured toughness. It was observed that the level of switching was dramatically reduced in the plasma treated joints that exhibited lower toughness. The weakened interface caused by these particular treatments encourages

Table 1 Tabulated Elemental Composition of Carbon, Oxygen, Nitrogen, Sulphur, and Silicon from Surveyed Spectra in Fig. 12

	Elemental composition (atomic %)				
Sample/Treatment	C	O	N	S	Si
Untreated	74.9	17.8	2.8	2.8	1.7
He/O_2 - 1250 W - 5 passes	65.0	24.2	6.5	3.2	1.1

Note the increase in percentage oxygen.

Table 2 Composition of Specific Functional Groups from Surveyed Spectra in Fig. 12

	% Composition (by curve fitting C 1s level)					
Sample/Treatment	C−C	C−O	C=O	COO	C* -C=O	π- π*
Untreated	67.7	25.1	0	0	0	7.2
He/O_2 - 1250 W - 5 Passes	41.8	37.6	3.0	2.3	7.9	7.4

Note the increase in oxygen containing functional groups.

the interfacial failure to remain predominantly on one beam as shown in Fig. 13. This is particularly noticeable for the specimens treated for 24 passes where the adhesive remains predominantly on one substrate. Note that this may also give the impression that the adhesive layer is thicker for the 5 min (12 pass) and 10 min (24 pass) treated joints in Fig. 13 compared to the untreated and two pass joint systems. However, the adhesive layer was found to be quite consistent between samples (≈ 0.25 mm).

Previous work published by Chen and Dillard [35] and Chen *et al*. [36] has shown how crack-path selection can lead to differences in the measured fracture toughness. The authors demonstrated that high levels of switching resulted in a higher toughness compared to the case when the adhesive remained on one substrate. It should be noted that this was due to variations in the T-stress as well as mode-mixity. However, the observations agree well with the present study.

A number of theories were explored as to the cause of the reduced toughness in the treated co-cured joints and various microscopy and thermal analysis techniques were used to explore these possibilities. Since plasma surface treatments have been shown to increase the detrimental effects of hygrothermal ageing [37], it was first considered that the highly polar surface attracted the water released during the cure cycle to the interface, thereby increasing the size and concentration of the interface voids.

It was also considered, based on previous work by the present authors [2], that by attracting the water to the interface, it would not enter the adhesive and reduce the glass transition temperature, T_g. Cross-sections of the adhesive-substrate interface from an untreated and a plasma-treated sample (He/O_2 at 1600 W for 24 passes) were prepared for SEM. These samples correspond to a Mode I fracture toughness, G_{IC}, of $883 \pm 128\,J/m^2$ and $626 \pm 122\,J/m^2$, respectively. The micrographs are shown in Fig. 14. It was observed that the size and number of the voids increased in the treated sample. It is likely that the higher concentration of voids would weaken the interface and reduce the fracture toughness of the joint.

Adhesive was taken from the fracture surfaces of the treated samples and T_g was determined. The results are presented in Fig. 15. It was observed that the glass transition temperature of the adhesive from the co-cured joints increased when the prepreg was plasma-treated. As mentioned previously,

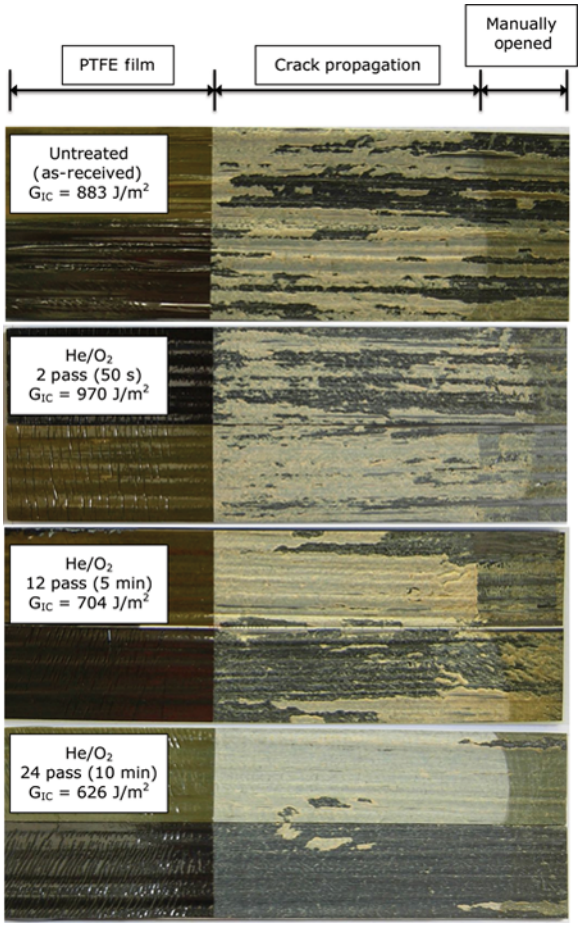

Figure 13 Fracture surfaces of various treated co-cured joints. The applied power was constant at 1600 W for all treatments. Regions corresponding to the PFTE film, crack propagation, and where the specimen was manually opened to allow for visual examination of the fracture surface have been highlighted. The fracture toughness values are those from Fig. 11.

this was possibly due to the water being attracted to the polar surface of the prepreg [37].

The plasma surface treatments may result in curing of the prepreg material either through heating of the sample or through plasma polymerisation of the prepreg surface. The level of heat-induced cure was investigated using DTA dynamic scans on the untreated and plasma-treated (He/O_2, 1600 W, 24 pass) bulk prepreg samples. It has been shown that the enthalpy of reaction is directly related to the quantity of unreacted epoxy endgroups [38]. No change in the degree of cure of the bulk materials was found using this method. While the APP system used in this study has been shown to

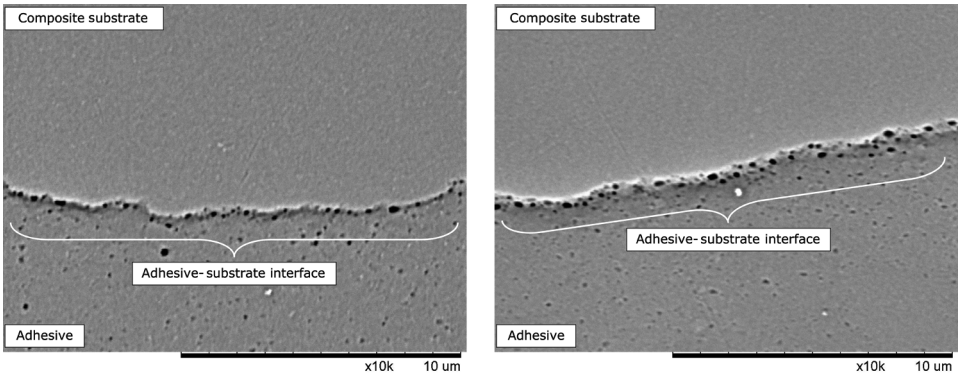

Figure 14 SEM images of adhesive-substrate interface for an untreated (G_{IC} = **883** J/m^2) and treated (**626** J/m^2) co-cured joint. Note the higher concentration of voids at the interface for the treated sample. The size of the voids has also increased. (a) Untreated. (b) He/O_2, 1600 W and 24 passes.

result in gas temperatures of 310 Kelvin (37°C) [27], this is unlikely to be sufficient to initiate polymerisation of a 180°C epoxy resin system. Any curing of the prepreg would likely be confined to the top few nanometers of the material. Previous studies using an Fourier transform infrared (FTIR) spectroscopy technique have demonstrated that plasmas can induce curing of liquid epoxy resins [39]. The drop in the dispersive component found in the current study (Fig. 5) may suggest some level of polymerisation of the prepreg surface [9,32]. Curing by this means is unlikely to result in full cure according to the manufacturers guidelines and may have contributed to the reduced fracture toughness for the 12 and 24 pass treated joint systems.

Plasma activation can also ablate [40] and oxidise [41] the surface of treated polymers leading to morphological changes [42]. It was also considered that for longer treatment times and/or higher applied powers,

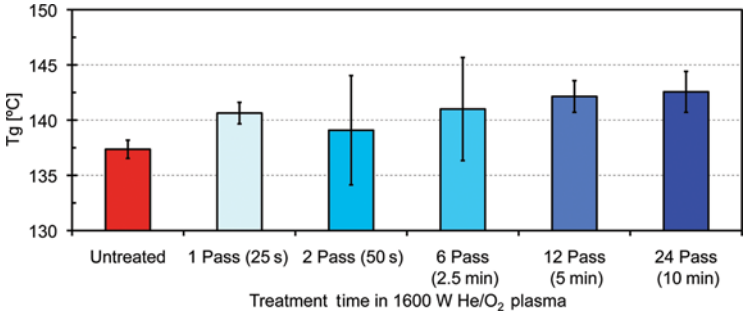

Figure 15 Glass transition temperature of adhesive taken from the surfaces of untreated and plasma treated co-cured joints.

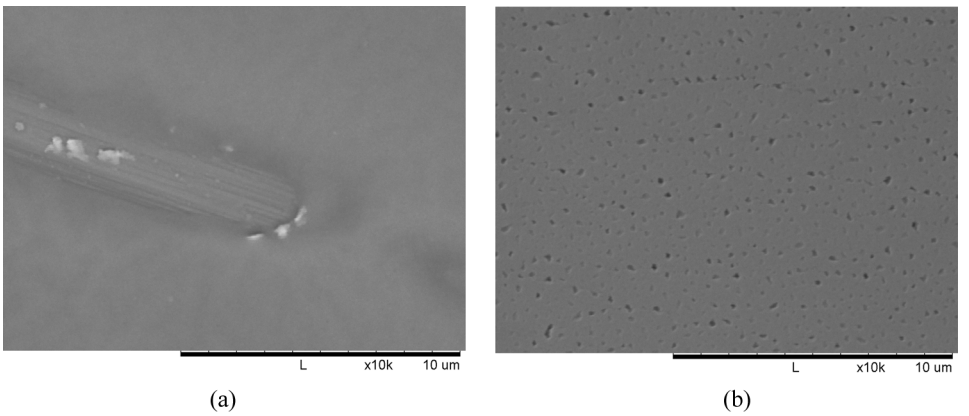

Figure 16 SEM image of the surface of (a) an untreated prepreg and (b) one treated with a He/O_2 plasma at 1750 W for 10 passes. (a) Untreated. (b) He/O_2, 1750 W, and 10 passes.

ablation of the prepreg surface may occur and lead to the development of a weakened boundary layer. SEM images of an untreated and a plasma treated prepreg are shown in Fig. 16. As before, note that the processing parameters were from a second experimental programme. Figure 16b shows evidence of pitting on the surface of the prepreg after the plasma treatment; this pitting is absent in the case of the untreated prepreg (Fig. 16a).

4. CONCLUSIONS

In this study, the prepreg material was treated with an atmospheric pressure plasma and its effect on the fracture toughness of the resulting co-cured joints was examined. Treatments of this type have previously been used for improving the delamination fracture toughness of laminates. In the present study, a modest improvement in fracture toughness of approximately 15–18% was achieved. However, as discussed previously, the error bars overlapped to a large extent (as can be seen in Fig. 11). Ideally, a change in the locus of failure from interfacial to cohesive would have been more conclusive.

A He/O_2 atmospheric pressure plasma treatment has been shown to be effective in increasing the surface energy of a carbon-fiber/epoxy prepreg and it was shown that these treatments are stable under ambient conditions for at least the shelf life of the material. In contrast, a He and He/N_2 plasma treatment were shown be very inefficient in increasing the surface energy. OES suggests it is the higher relative quantity of oxygen-containing species in the He/O_2 plasma that are important for improving the surface energy. The XPS analysis supports this by verifying the introduction of oxygen-containing functional groups onto the surface of the prepreg.

It was shown that excessive treatments can lead to a severe degradation in the performance of the co-cured joint system under Mode I loading conditions. Microscopy and thermal analysis were used to explain these results in Section 3.4. It was observed that the adhesive-substrate interface contained a larger concentration of voids when treated for 24 passes at 1600 W in a He/O_2 plasma. It was proposed that the highly polar surface attracted the moisture to the interface. This was supported by an increase in the glass transition temperature of the adhesive layer. Scanning electron microscopy of the treated prepreg revealed pitting on the surface after excessive plasma treatments. Any one of these effects could possibly lead to a reduction in fracture toughness. It is likely the reduced toughness is a combination all the factors investigated.

ACKNOWLEDGEMENTS

The materials provided by Cytec Engineered Materials (CEM) are gratefully acknowledged.

FUNDING

The authors would like to gratefully acknowledge the financial support of the Irish Research Council for Science, Engineering and Technology (IRCSET), Irish Centre for Composites Research (IComp), and Cytec Engineered Materials (CEM).

REFERENCES

[1] Zhou, J. and Lucas, J. P., Hygrothermal effects of epoxy resin. Part I: the nature of water in epoxy. *Polymer* **40**, 5505–5512 (1999).

[2] Mohan, J., Ivankovic, A., and Murphy, N., Effect of prepreg storage humidity on the mixed-mode fracture toughness of a co-cured composite joint. *Composites Part A: Applied Science and Manufacturing* **45**, 23–34 (2013).

[3] Mohan, J., An Investigation of composite-to-composite bonding, Ph.D. Thesis, School of Electrical, Electronic & Mechanical Engineering, University College Dublin, Ireland (2010).

[4] Liston, E. M., Plasma treatment for improved bonding: A review. *The Journal of Adhesion* **30**, 199–218 (1989).

[5] Chin, J. W. and Wightman, J. P., Surface characterization and adhesive bonding of toughened bismaleimide composites. *Composites: Part A* **27A**, 419–428 (1996).

[6] Comyn, J., Mascia, L., Xiao, G., and Parker, B. M., Plasma-treatment of polyetheretherketone (PEEK) for adhesive bonding. *International Journal of Adhesion and Adhesives* **16**, 97–104 (1996).

[7] Comyn, J., Mascia, L., Xiao, G., and Parker, B. M., Corona-discharge treatment of polyetheretherketone (PEEK) for adhesive bonding. *International Journal of Adhesion and Adhesives* **16**, 301–304 (1996).
[8] Wade, G. A. and Cantwell, W. J., Adhesive bonding and wettability of plasma treated, glass fiber-reinforced nylon-6,6 composites. *Journal of Material Science Letters* **19**, 1829–1832 (2000).
[9] Kusano, Y., Mortensen, H., Stenum, B., Kingshott, P., Andersen, T. L., Brondsted, P., Bilde-Sørensen, J. B., Sørensen, B. F., and Bindslev, H., Atmospheric pressure plasma treatment of glass fiber composite for adhesion improvement. *Plasma Processes and Polymers* **4** (S), 455–459 (2007).
[10] Shanahan, M. E. R. and Bourges-Monnier, C., Effects of plasma treatment on the adhesion of an epoxy composite. *International Journal of Adhesion and Adhesives* **16**, 129–135 (1996).
[11] Kim, J. K. and Lee, D. G., Characteristics of plasma surface treated composite adhesive joints at high environmental temperature. *Composite Structures* **57**, 37–46 (2002).
[12] Kim, J. K., Kim, H. S., and Lee, D. G., Adhesion characteristics of carbon/epoxy composites treated with low- and atmospheric pressure plasmas. *Journal of Adhesion Science and Technology* **17** (13), 1751–1771 (2003).
[13] Kim, J. K. and Lee, D. G., Adhesion characteristics of plasma surface treated carbon/epoxy composite. *Journal of Adhesion Science and Technology* **17** (7), 1017–1037 (2003).
[14] Fischer, F., Kreling, S., Jaschke, P., Frauenhofer, M., Kracht, D., and Dilger, K., Laser surface pre-treatment of CFRP for the adhesive bonding in consideration of the absorption behaviour. *The Journal of Adhesion* **88**, 350–363 (2012).
[15] Prolongo, S. G., Gude, M. R., Sanchez, J., and Urena, A., Nanoreinforced epoxy adhesives for aerospace industry. *The Journal of Adhesion* **85**, 180–199 (2009).
[16] Kinloch, A. J., Kodokian, G. K. A., and Watts, J. F., The adhesion of thermoplastic fiber composites. *Philosophical Transactions: Physical Sciences and Engineering* **338**, 83–112 (1992).
[17] Kim, M. H., Rhee, K. Y., Paik, Y. N., and Ryu, S. H., A study on the fracture characteristics of plasma-treated graphite/epoxy laminated composites. *Key Engineering Materials* **321–323**, 869–872 (2006).
[18] BS-7991-2001. Determination of the Mode I Adhesive Fracture Energy, G_{IC}, of structural adhesives using the double cantilever beam (DCB) and tapered double cantilever beam (TDCB) specimens, 2001.
[19] Williams, J. G., On the calculation of energy release rates for cracked laminates. *International Journal of Fracture* **36**, 101–119 (1988).
[20] Williams, J. G., The fracture mechanics of delamination tests. *Journal of Strain Analysis* **24** (4), 207–214 (1989).
[21] Hashemi, S., Kinloch, A. J., and Williams, J. G., The analysis of interlaminar fracture in uniaxial fiber-polymer composites. *Proceedings of the Royal Society of London* **427**, 173–199 (1990).
[22] Owens, D. K. and Wendt, R. C., Estimation of the surface free energy of polymers. *Journal of Applied Polymer Science* **13**, 1741–1747 (Aug. 1969).

[23] Strom, G., Fredriksson, M., and Stenius, P., Contact angles, work of adhesion, and interfacial tensions at a dissolving hydrocarbon surface. *Journal of Colloid and Interface Science* **119**, 352–361 (1987).
[24] Strobel, M. and Lyons, C. S., An essay on contact angle measurements. *Plasma Processes and Polymers* **8**, 8–13 (2011).
[25] Muller, M. and Oehr, C., Comments on 'An essay on contact angle measurements'. *Plasma Processes and Polymers* **8**, 19–24 (2011).
[26] Dowling, D. P., Twomey, B., and Byrne, G., Deposition of functional coatings using an in-line atmospheric pressure plasma apparatus, in Society of Vacuum Coaters 48th Annual Technical Conference Proceedings (2005).
[27] Twomey, B., Nindrayog, A., Niemi, K., Graham, W. G., and Dowling, D. P., Correlation between the electrical and optical properties of an atmospheric pressure plasma during siloxane coating deposition. *Plasma Chemistry and Plasma Processing* **31**, 139–156, (2011).
[28] Hino, T., Yamauchi, Y., Ono, J., and Hirohata, Y., Enhancement of reactive species density in nitrogen plasma by mixture of helium and nitridation experiment for silicon. *Vacuum* **74**, 467–471 (2004).
[29] Cvelbar, U., Krstulovic, N., Milosevic, S., and Mozetic, M., Inductively coupled RF oxygen plasma characterization by optical emission spectroscopy. *Vacuum* **82**, 224–227 (2008).
[30] Twomey, B., Rahman, M., Byrne, G., Hynes, A., OHare, L. A., O'Neill, L., and Dowling, D. P., Effect of plasma exposure on the chemistry and morphology of aerosol-assisted, plasma-deposited coatings. *Plasma Processes and Polymers* **5**, 737–744 (2008).
[31] Kim, J. Y., Lee, D. H., Ballato, J., Cao, W., and Kim, S. O., Reactive oxygen species controllable non-thermal helium plasmas for evaluation of plasmid DNA strand breaks. *Applied Physics Letters* **101**, 1–5 (2012).
[32] Arpagaus, C., Rossi, A., and von Rohr, Ph. R., Short-time plasma surface modification of HDPE powder in a Plasma Downer Reactor process, wettability improvement and ageing effects. *Applied Surface Science* **252**, 1581–1595 (2005).
[33] Twomey, B., *The deposition of siloxane coatings using an atmospheric pressure plasma system*. Ph.D. Thesis, School of Electrical, Electronic & Mechanical Engineering, University College Dublin, Ireland (2008).
[34] Seidel, C., Kopf, H., Gotsmann, B., Vieth, T., Fuchs, H., and Reihs, K., Ar plasma treated and Al metallised polycarbonate: A XPS, mass spectroscopy and SFM study. *Applied Surface Science* **40**, 19–33 (1999).
[35] Chen, B. and Dillard, D. A., The effect of the T-stress on crack path selection in adhesively bonded joints. *International Journal of Adhesion and Adhesives* **21**, 357–368 (2001).
[36] Chen, B., Dillard, D. A., Dillard, J. G., and Clark, Jr. R. L., Crack path selection in adhesively bonded joints: The roles of external loads and speciment geometry. *International Journal of Fracture* **114**, 167–190 (2002).
[37] Gude, M. R., Prolongo, S. G., and Urena, A., Hygrothermal ageing of adhesive joints with nanoreinforced adhesives and different surface treatments of carbon fiber/epoxy substrates. *International Journal of Adhesion and Adhesives* **40**, 179–187 (2013).

[38] Varley, R. J., Hodgkin, J. H., Hawthorne, D. G., Simon, G. P., and McCulloch, D., Toughening of a trifunctional epoxy system Part III. Kinetic and morphological study of the thermoplastic modified cure process. *Polymer* **41**, 3425–3436 (2000).

[39] Kondyurin, A. and Lauke, B., Curing of liquid epoxy resin in plasma discharge. *European Polymer Journal* **40**, 1915–1923 (2004).

[40] Park, J. K., Ju, W. T., Paek, K. H., Kim, Y. H., Choi, Y. H., Kim, J. H., and Hwang, Y. S., Pre-treatments of polymers by atmospheric pressure ejected plasma for adhesion improvement. *Surface and Coatings Technology* **174–175**, 547–552 (2003).

[41] Mozetic, M., Controlled oxidation of organic compounds in oxygen plasma. *Vacuum* **71**, 237–240 (2003).

[42] Li, H., Liang, H., He, F., Huang, Y., and Wan, Y., Air dielectric barrier discharges plasma surface treatment of three-dimensional braided carbon fiber reinforced epoxy composites. *Surface and Coating Technology* **203** (10–11), 1317–1321 (2009).